RNA Interference-Mediated Repression of *MtCCD1* in Mycorrhizal Roots of *Medicago truncatula* Causes Accumulation of C_{27} Apocarotenoids, Shedding Light on the Functional Role of CCD1[1][W][OA]

Daniela S. Floss, Willibald Schliemann, Jürgen Schmidt, Dieter Strack, and Michael H. Walter*

Leibniz-Institut für Pflanzenbiochemie, Abteilung Sekundärstoffwechsel (D.S.F., W.S., D.S., M.H.W.) and Abteilung Natur- und Wirkstoffchemie (J.S.), D–06120 Halle (Saale), Germany

Tailoring carotenoids by plant carotenoid cleavage dioxygenases (CCDs) generates various bioactive apocarotenoids. Recombinant CCD1 has been shown to catalyze symmetrical cleavage of C_{40} carotenoid substrates at 9,10 and 9′,10′ positions. The actual substrate(s) of the enzyme in planta, however, is still unknown. In this study, we have carried out RNA interference (RNAi)-mediated repression of a *Medicago truncatula CCD1* gene in hairy roots colonized by the arbuscular mycorrhizal (AM) fungus *Glomus intraradices*. As a consequence, the normal AM-mediated accumulation of apocarotenoids (C_{13} cyclohexenone and C_{14} mycorradicin derivatives) was differentially modified. Mycorradicin derivatives were strongly reduced to 3% to 6% of the controls, while the cyclohexenone derivatives were only reduced to 30% to 47%. Concomitantly, a yellow-orange color appeared in RNAi roots. Based on ultraviolet light spectra and mass spectrometry analyses, the new compounds are C_{27} apocarotenoic acid derivatives. These metabolic alterations did not lead to major changes in molecular markers of the AM symbiosis, although a moderate shift to more degenerating arbuscules was observed in RNAi roots. The unexpected outcome of the RNAi approach suggests C_{27} apocarotenoids as the major substrates of CCD1 in mycorrhizal root cells. Moreover, literature data implicate C_{27} apocarotenoid cleavage as the general functional role of CCD1 in planta. A revised scheme of plant carotenoid cleavage in two consecutive steps is proposed, in which CCD1 catalyzes only the second step in the cytosol ($C_{27} \rightarrow C_{14} + C_{13}$), while the first step ($C_{40} \rightarrow C_{27} + C_{13}$) may be catalyzed by CCD7 and/or CCD4 inside plastids.

Carotenoids are a large class of isoprenoid pigments, which are produced by plants and certain microbes. Conjugated double bonds in a C_{40} tetraterpene skeleton form the basis of their chromophores, which are extended and modified by cyclization, isomerization, and oxidation. Carotenoids fulfill important roles as accessory photosynthetic pigments harvesting light and preventing photooxidative damage, as general antioxidants, and as mediators of membrane fluidity. They also serve as yellow, orange, and red pigments in many flowers and fruits. In plants, biosynthesis of C_{40} carotenoids is compartmentalized to plastids, comprising not only chloroplasts but also chromoplasts and other plastid types (Hirschberg, 2001). A plastidial location also applies for the early steps of biosynthesis carried out by enzymes of the methylerythritol phosphate (MEP) pathway, generating C_5 isopentenyl diphosphate precursors (Rodríguez-Concepción and Boronat, 2002).

Carotenoid catabolism is not simply responsible for balancing steady-state carotenoid levels but forms many new bioactive compounds. While unspecific chemical oxidative cleavage is possible, the vast majority of known cleavage products (apocarotenoids) are thought to originate from defined cleavage ("tailoring") of carotenoids by carotenoid cleavage dioxygenase (CCD) enzymes (Giuliano et al., 2003; Bouvier et al., 2005; Auldridge et al., 2006b; Kloer and Schulz, 2006). CCDs display a high degree of regiospecificity and stereospecificity and give rise to a variety of different products with a multitude of biological functions. These include the widespread C_{13} apocarotenoid volatiles of flower scents and fruit aromas from rose (*Rosa* spp.), tomato (*Solanum lycopersicum*), melon (*Cucumis melo*), and many others (Eugster and Märki-Fischer, 1991; Lewinsohn et al., 2005) and the C_{20}, C_{24}, and C_{10} colorants and spices of annatto (*Bixa orellana*) and saffron (*Crocus sativus*; Bouvier et al., 2005). In addition, many signaling molecules comprising abscisic acid (ABA), strigolactones, and a shoot-branching inhibitor with unknown structure are derived from cleavage products of carotenoids (Akiyama et al., 2005;

[1] This work was supported in part by the Deutsche Forschungsgemeinschaft (Bonn) in the priority program SPP 1084 (MolMyk).

* Corresponding author; e-mail mhwalter@ipb-halle.de.

The author responsible for distribution of materials integral to the findings presented in this article in accordance with the policy described in the Instructions for Authors (www.plantphysiol.org) is: Michael H. Walter (mhwalter@ipb-halle.de).

[W] The online version of this article contains Web-only data.

[OA] Open Access articles can be viewed online without a subscription.

www.plantphysiol.org/cgi/doi/10.1104/pp.108.125062

Nambara and Marion-Poll, 2005; Mouchel and Leyser, 2007).

Molecular identification has by now defined nine different clades of plant CCDs, which are named after their representatives in Arabidopsis (*Arabidopsis thaliana*). AtCCD1, AtCCD4, AtCCD7, and AtCCD8 cleave a variety of trans-carotenoid substrates at specific double bonds, but only CCD1 and CCD7 have confirmed cleavage specificities. Recombinant AtCCD1 cleaves symmetrically at 9,10 (9′,10′) positions to yield two C_{13} ketones and one C_{14} dialdehyde from one C_{40} parent carotenoid molecule (Schwartz et al., 2001; Fig. 1). Recently, additional in vitro activity of CCD1 on 5,6 (5′,6′) double bonds of lycopene has been reported (Vogel et al., 2008). Recombinant AtCCD7 exhibits regioselectivity for the 9,10 position similar to AtCCD1, yet it cleaves only once asymmetrically, resulting in C_{13} and C_{27} products (Schwartz et al., 2004). AtCCD8 seems to further cleave this C_{27} product to C_{18} and C_9, which are the assumed precursors of a still elusive shoot-branching inhibitor (Schwartz et al., 2004; Alder et al., 2008). While these four CCD classes are structurally only distantly related to each other, the remaining five CCDs fall into one class of specialized CCDs. These are called NCEDs, a term derived from their specificity for 9-cis-epoxycarotenoid substrates. Arabidopsis NCED2, NCED3, NCED5, NCED6, and NCED9 are all related to VP14, the prototype NCED/CCD characterized first from the maize (*Zea mays*) mutant *vp14*, which is impaired in the earliest step of ABA biosynthesis from carotenoids (Schwartz et al., 1997; Tan et al., 2003). All NCEDs cleave the 11,12 double bond of 9-cis isomers of neoxanthin or violaxanthin to yield the ABA precursor xanthoxin. Import studies, immunolocalization experiments, and transit peptide prediction algorithms suggest a plastidial location for all NCEDs and CCDs except CCD1, which has been shown in several plant systems to act in the cytosol (Bouvier et al., 2003; Tan et al., 2003; Simkin et al., 2004a; Auldridge et al., 2006a).

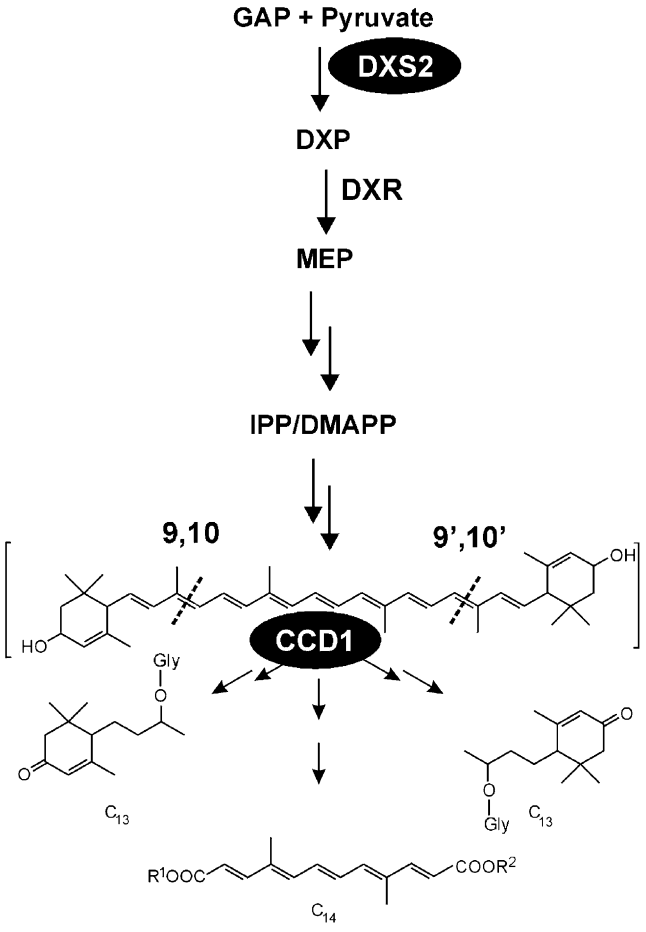

Figure 1. Simplified hypothetical pathway to C_{13} cyclohexenone and C_{14} mycorradicin derivatives in mycorrhizal roots. The indicated cleavage specificities of CCD1 and its presumed C_{40} carotenoid substrate have been deduced from in vitro studies. An early biosynthetic step in the MEP pathway previously targeted for gene silencing (DXS2) is highlighted. The carotenoid precursor in mycorrhizal roots is still elusive. DMAPP, Dimethylallyl diphosphate; DXP, 1-deoxy-D-xylulose 5-phosphate; DXR, 1-deoxy-D-xylulose 5-phosphate reductoisomerase; GAP, glyceraldehyde 3-phosphate; Gly, glycoside; IPP, isopentenyl diphosphate; MEP, 2-*C*-methyl-D-erythritol 4-phosphate; R^1, R^2, unknown moieties.

Root colonization by arbuscular mycorrhizal (AM) fungi frequently leads to the accumulation of large amounts of apocarotenoids of a cyclic C_{13} type and a linear C_{14} type (Klingner et al., 1995; Maier et al., 1995; Walter et al., 2000; Strack and Fester, 2006; Fig. 1). This phenomenon occurs preferentially during late stages of the AM symbiotic plant-microbe interaction and is often accompanied by the appearance of a yellowish root coloration. The chromophore responsible for this coloration is mycorradicin, a C_{14} polyenic dicarboxylic acid. Derivatives of mycorradicin accumulate concomitantly with structural variants of C_{13} cyclohexenones, the latter being glycosylated and deposited in vacuoles. Both of these AM-induced apocarotenoid types were predicted to be generated by the action of a CCD1-type enzyme on a common C_{40} carotenoid precursor (Walter et al., 2000, 2007; Hans et al., 2004; Strack and Fester, 2006; Akiyama, 2007; Fig. 1). Attempts to isolate pathway intermediates and particularly the proposed C_{40} carotenoid precursor have so far only led to the detection of a minor increase in phytoene upon application of the carotenoid biosynthesis inhibitor norfluorazon (Fester et al., 2005). This indicates that carotenoid cleavage is unlikely to be a rate-limiting step in the biosynthesis of these apocarotenoids in mycorrhizal roots and that the carotenoids formed during the symbiosis are probably instantly cleaved. A different class of plant apocarotenoids (strigolactones) occurring in low quantities plays a role in early signaling steps of the AM symbiosis (Akiyama et al., 2005; Matusova et al., 2005), but whether there is any relationship to the biogenesis of abundant C_{13}- and C_{14}-type apocarotenoids is currently unknown.

Previous molecular studies on the accumulation of C_{13} and C_{14} apocarotenoids in mycorrhizal roots have focused on the first two steps of the MEP pathway. Both *1-deoxy-D-xylulose 5-phosphate synthase* (*DXS*) and *1-deoxy-D-xylulose 5-phosphate reductoisomerase* genes were shown to be transcriptionally up-regulated in cereal roots upon mycorrhization, emphasizing the importance of precursor supply activation (Walter et al., 2000; Hans et al., 2004). Further investigations revealed the widespread occurrence of two differentially regulated *DXS* isogenes, of which only *DXS2* was up-regulated in mycorrhizal roots (Walter et al., 2002). Recent studies have shown local promoter activity of a *DXS2* gene in cells hosting fungal arbuscules (Floss et al., 2008), in accordance with earlier findings of local apocarotenoid deposition in arbusculated cells (Fester et al., 2002a).

Arbuscules are highly branched fungal organs outgrowing from hyphae within host cortical root cells, which constitute the predominant site of nutrient exchange between the plant and the fungal symbiont. Their proper function can determine the development of symbiotic structures (Javot et al., 2007). Interestingly, strong silencing of *DXS2* expression in hairy roots of *Medicago truncatula* leads to reduced levels of both types of apocarotenoids (cyclohexenone and mycorradicin derivatives), accompanied by an abolishment of the normal expression of many arbuscule-specific plant marker genes (Floss et al., 2008). However, whether this impairment of symbiotic functions is indeed linked to the lack of either of these mycorrhizal apocarotenoids is still unresolved, since effects from the absence of other *DXS2*-dependent isoprenoids cannot be excluded.

This still inconclusive result led us to target the later steps in the pathway, namely carotenoid cleavage, for a new RNA interference (RNAi) approach to elucidate the function of C_{13} cyclohexenone and/or C_{14} mycorradicin apocarotenoids in the AM symbiosis. *CCD1* genes have been characterized from several plants, all showing that in *Escherichia coli* recombinant CCD1 preferentially cleaves a variety of C_{40} carotenoids with cyclic and noncyclic end groups symmetrically at the 9,10 (9′,10′) double bonds (Schwartz et al., 2001; Mathieu et al., 2005; Ibdah et al., 2006; Fig. 1). However, it has not been proven whether these biochemical cleavage properties in vitro also represent the normal biological role of CCD1 enzymes. In fact, little is known about the actual substrates of native CCD1 in compartmentalized plant cells containing plastids. Previous knockdown approaches on *CCD1* expression in transgenic plants have resulted in strong suppression of *CCD1* transcript levels but to only limited effects on C_{40} carotenoid levels, prompting speculations about additional players (Simkin et al., 2004a, 2004b; Auldridge et al., 2006a). In this study, we have silenced the expression of a *MtCCD1* gene in mycorrhizal hairy roots of *M. truncatula*. Surprisingly, the accumulation of the two hitherto known mycorrhiza-induced apocarotenoid types was reduced to different extents and novel C_{27} apocarotenoid derivatives appeared as a consequence of *MtCCD1* repression. Together, these and other observations lead to a new view of carotenoid cleavage in planta, reconciling previous contradictions regarding the presumed substrate and the CCD1 enzyme being in different cellular compartments.

RESULTS

Cloning of a *MtCCD1* cDNA and Proof of Functionality of the Protein Encoded

A full-length *MtCCD1* cDNA was isolated from a *M. truncatula* mycorrhizal root cDNA library using an 825-bp *MtCCD1* fragment as a probe. DNA sequencing of several clones revealed complete identity of the cDNA (accession no. FM204879) to TC100912 of the Dana-Farber Cancer Institute (DFCI) Medicago Gene index (http://compbio.dfci.harvard.edu/tgi/cgi-bin/tgi/gimain.pl?gudb=medicago). The deduced MtCCD1 protein consists of 540 amino acids and has a calculated molecular mass of 60.9 kD. The MtCCD1 amino acid sequence exhibits strong similarity to many other CCD1 proteins, exemplified by 87.2% identity (91.1% similarity) to *Phaseolus vulgaris* CCD1, 80.2% identity (86.8% similarity) to Arabidopsis CCD1, and 76.5% identity (82.8% similarity) to maize CCD1 (Supplemental Fig. S1). This indicates that MtCCD1 belongs to the well-studied class of CCD1 proteins and genes (Schwartz et al., 2001; Simkin et al., 2004a, 2004b; Mathieu et al., 2005; Auldridge et al., 2006a; Ibdah et al., 2006; Kato et al., 2006; Sun et al., 2008; Vogel et al., 2008; Supplemental Fig. S1). Application of prediction algorithms (http://www.cbs.dtu.dk/services/) suggests a subcellular localization of the MtCCD1 protein in the cytosol, in accordance with reports on other CCD1 proteins (data not shown). Searching EST databases of *M. truncatula* revealed 29 ESTs of the *MtCCD1* type from all kinds of tissues, including roots and mycorrhizal roots. Four types of *MtCCD1*-related ESTs of 83% to 86% deduced amino acid sequence identity to MtCCD1 transcribed from putative *MtCCD1* paralogs were much less abundant (one to three ESTs each) and originated from pod or shoot libraries but not from roots.

To prove the functionality of the protein encoded in the *MtCCD1* cDNA, two constructs with or without a His tag were expressed in *E. coli* cells engineered to produce β-carotene (pAC-BETA) or zeaxanthin (pAC-ZEAX; Cunningham et al., 1996; Sun et al., 1996). Using both constructs, a MtCCD1 protein band of the calculated size could be observed after induction by isopropyl β-D-1-thiogalactopyranoside and separation on SDS gels. The expression of both constructs led to the expected decoloration of the two carotenogenic *E. coli* strains, which was absent in controls expressing the empty vector (EV) pET28a (Fig. 2). This demonstrates carotenoid cleavage activity of the recombinant protein encoded in the *MtCCD1* cDNA.

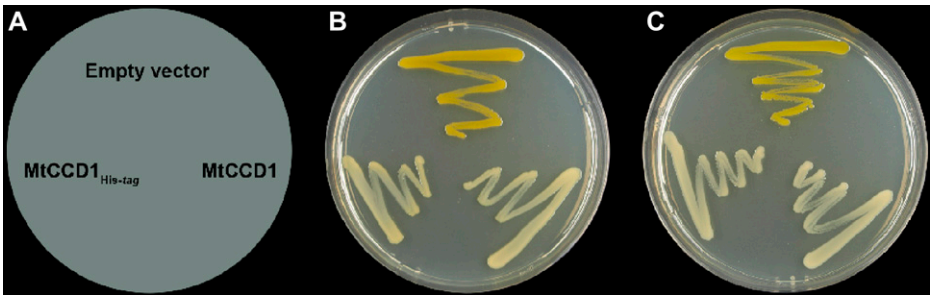

Figure 2. Expression of the *MtCCD1* cDNA in *E. coli* strains engineered for carotenoid production. *MtCCD1* expression constructs in pET-28a lacking or containing a C-terminal His tag as indicated were introduced into *E. coli* strains containing the plasmid pAC-BETA (center) or pAC-ZEAX (right) for β-carotene or zeaxanthin formation, respectively. The streak on top represents the strain transformed with the EV control.

Up-Regulation of *MtCCD1* Transcript Levels in Mycorrhizal Roots of *M. truncatula*

Previous analyses have indicated a minor to moderate up-regulation of *CCD1* transcripts in roots upon colonization by mycorrhizal fungi for both *M. truncatula* and maize (Lohse et al., 2005; Sun et al., 2008). To confirm these results for this study, we conducted an AM fungal colonization experiment on wild-type roots of *M. truncatula* for 7 and 9 weeks and for several biological replicates. An early gene of apocarotenoid biosynthesis, known to be AM inducible (*MtDXS2*; Walter et al., 2002; Floss et al., 2008), and a molecular marker of mycorrhizal colonization (the AM-specific expression of the phosphate transporter gene *MtPT4*; Harrison et al., 2002) were included in the analysis. Although *MtCCD1* transcript levels were not elevated as strongly as those of either *MtDXS2-1* or *MtPT4*, they exhibited a slight increase after 7 weeks and a still minor but significant elevation after 9 weeks (3-fold) in mycorrhizal roots compared with nonmycorrhizal control roots (Table I). As discussed previously for *ZmCCD1*, local induction of *MtCCD1* transcript levels in arbusculated cells, the site of mycorrhizal apocarotenoid biosynthesis, is likely to be considerably higher than the induction factor calculated from extracts (Sun et al., 2008).

Knockdown of *MtCCD1* Expression Leads to Strong Reduction of Mycorradicin Derivatives But to Only Moderate Reduction of Cyclohexenone Derivatives

To reduce the levels of *MtCCD1* transcripts and thereby generate a loss-of-function mutant of *MtCCD1*, an RNAi construct of 335 bp covering the 3′ part of the coding region and 3′ untranslated sequences was generated. After transfer into the binary vector pRedRoot, this construct was introduced and expressed in transgenic hairy roots of *M. truncatula*. Concomitantly, plants expressing EV sequences were cultivated as controls. After injection of *Agrobacterium rhizogenes* transgene carriers into hypocotyls, further cultivation of plants involved the selection of transgenic roots outgrowing from the injection site and the removal of residual wild-type as well as untransformed hairy roots to obtain individual, independently transformed composite plants, each with individual transgenic hairy roots and a wild-type shoot.

Figure 3 summarizes the results of two experiments comparing mycorrhizal RNAi root samples with mycorrhizal EV control roots after 7 or 9 weeks of colonization. While the average levels of EV controls differed somewhat between the experiments, a strong reduction was observed in *MtCCD1* transcript levels in RNAi roots compared with EV control roots, resulting in about 8% residual transcripts in RNAi roots (Fig. 3A). Next, we determined the levels of both C_{14} mycorradicin and C_{13} cyclohexenone derivatives in these roots. Mycorradicin derivative concentrations were strikingly lower in RNAi roots (5 nmol g^{-1} fresh weight [7 weeks of colonization] and 3 nmol g^{-1} fresh weight [9 weeks of colonization]), corresponding to 6% and 3% residual levels of the amounts of EV controls (Fig. 3B). These reductions were thus in the same order of magnitude as the reduction in *MtCCD1* transcript levels, suggesting a link between MtCCD1 activity and the accumulation of mycorradicin derivatives. However, C_{13} cyclohexenone derivative levels were not

Table I. *Transcript levels of MtCCD1 in extracts of nonmycorrhizal and mycorrhizal wild-type roots after 7 or 9 weeks of fungal colonization by G. intraradices as determined by real time RT-PCR from three biological replicates*

For comparison, additional data were obtained from a gene involved in early steps of apocarotenoid biosynthesis (*MtDXS2-1*) and from an arbuscule molecular marker gene (*MtPT4*).

Time	Gene	$E^{\Delta Ct} \times 10^{-3}$	
		Nonmycorrhizal	Mycorrhizal
7 weeks	*MtCCD1*	28.0 ± 7.8	41.7 ± 14.6
	MtDXS2-1	7.6 ± 3.1	16.3 ± 4.0
	MtPT4	0.02 ± 0.005	273.3 ± 94.5
9 weeks	*MtCCD1*	20.7 ± 6.8	62.3 ± 21.5
	MtDXS2-1	4.4 ± 1.7	32.3 ± 5.1
	MtPT4	0.03 ± 0.01	825.3 ± 386.9

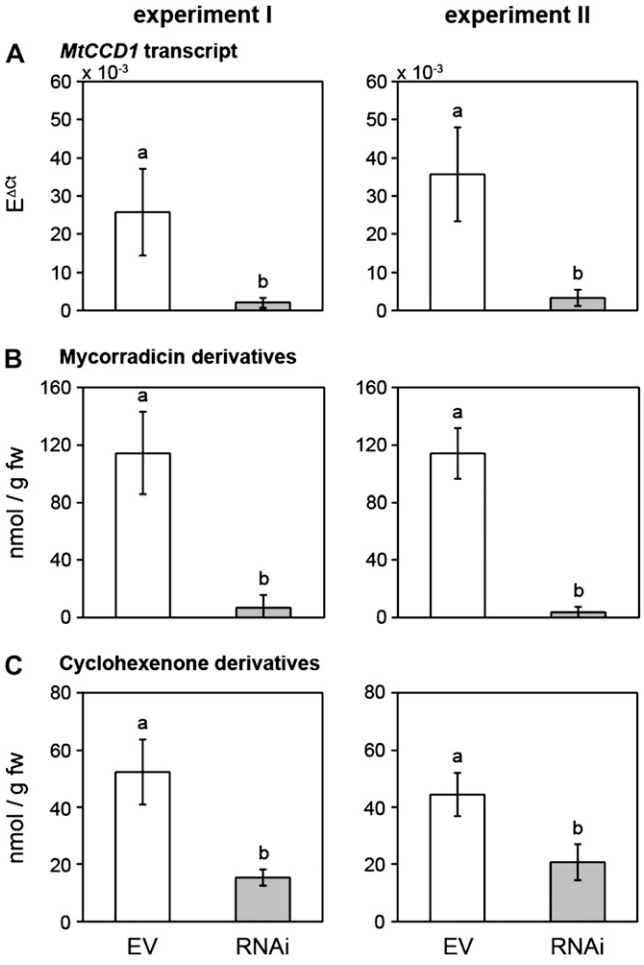

Figure 3. Transcript levels of *MtCCD1* and levels of mycorradicin and cyclohexenone derivatives in mycorrhizal hairy roots of *M. truncatula* reduced for *MtCCD1* expression. Results from two extensive experiments of two different colonization periods are shown using EV control roots (white columns) or RNAi roots (gray columns). The 7-week experiment consisted of eight individual EV controls and eight individual RNAi plants, while nine EV plants and 13 RNAi plants were used for the 9-week experiment. A, *MtCCD1* transcript levels were determined by real time RT-PCR. B and C, Mycorradicin (B) and cyclohexenone (C) derivatives were assigned by their characteristic UV light spectra and quantified by HPLC using external standards. Letters differing between columns indicate significant differences of means based on Kruskal-Wallis test (mycorradicin) or one-way test (cyclohexenone derivatives). fw, Fresh weight.

reduced to a comparable extent. They exhibited a significant reduction in both experiments, but the residual levels in RNAi roots compared with EV control roots were still between 30% and 47% on average (Fig. 3C).

A Yellow-Orange Root Coloration Appears in *MtCCD1*-Repressed Roots

In addition to the biochemical changes in the levels of the C_{13} and C_{14} apocarotenoids, the roots of the mycorrhizal RNAi plants exhibited a striking phenotypic change in coloration (Fig. 4). The EV control roots also exhibit a coloration, related to mycorradicin accumulation, but this orange-brown color is typically rather faint. It is similarly observed with mycorrhizal wild-type roots of *M. truncatula* (Walter et al., 2007). However, the RNAi roots silenced for *MtCCD1* expression exhibited a conspicuous change in color from the regular faint coloration in EV controls to a much more intense yellow-orange color in RNAi roots (Fig. 4). This indicates the accumulation of a compound(s) with a new chromophore caused by the absence of MtCCD1 activity. Change of root color was the only phenotypical change observed in the composite plants with *MtCCD1*-silenced roots. There were no differences in shoot or root biomass, flowering, seed set, or other plant growth parameters between plants with mycorrhizal RNAi roots or mycorrhizal EV control roots (data not shown).

HPLC and Mass Spectrometry Analyses Indicate Accumulation of C_{27} Apocarotenoid Derivatives in *MtCCD1*-Silenced Roots

Methanolic extracts of EV control roots and RNAi roots exhibiting a yellow to yellow-orange coloration were subjected to HPLC analyses. Using detection at 440 nm, at least seven new compounds were recognized in the mycorrhizal RNAi roots. (Fig. 5). They could not be detected in mycorrhizal EV controls (Fig. 5A) or in nonmycorrhizal RNAi roots (Fig. 5B). Analysis of roots from several individual transgenic root systems indicated a similar general pattern of accumulation but with variable proportions of the new compounds (Fig. 5B). Their UV spectra exhibited absorption maxima between 418 and 445 nm resembling those of recently described C_{27} apocarotenoids, which are known to be yellow-orange (Fig. 5A; Yokoyama and White, 1966; Cooper et al., 2003). None of these compounds exhibited UV light absorption signatures

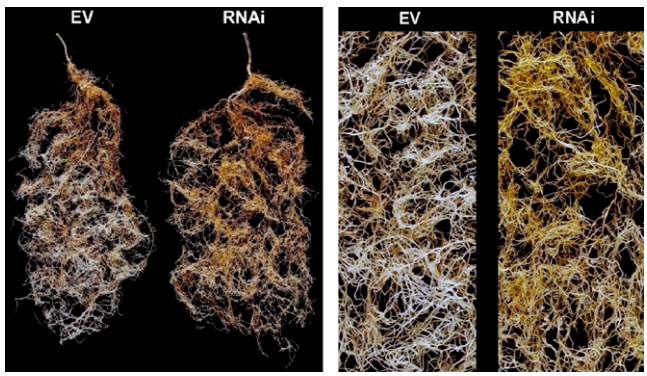

Figure 4. Conspicuous alteration of root color in mycorrhizal hairy roots reduced for *MtCCD1* expression. Total root systems or enlarged sectors of roots after 7 weeks of fungal colonization show faint orange-brown coloration of EV controls (left) or a much more intense yellow-orange coloration of *MtCCD1* RNAi roots (right).

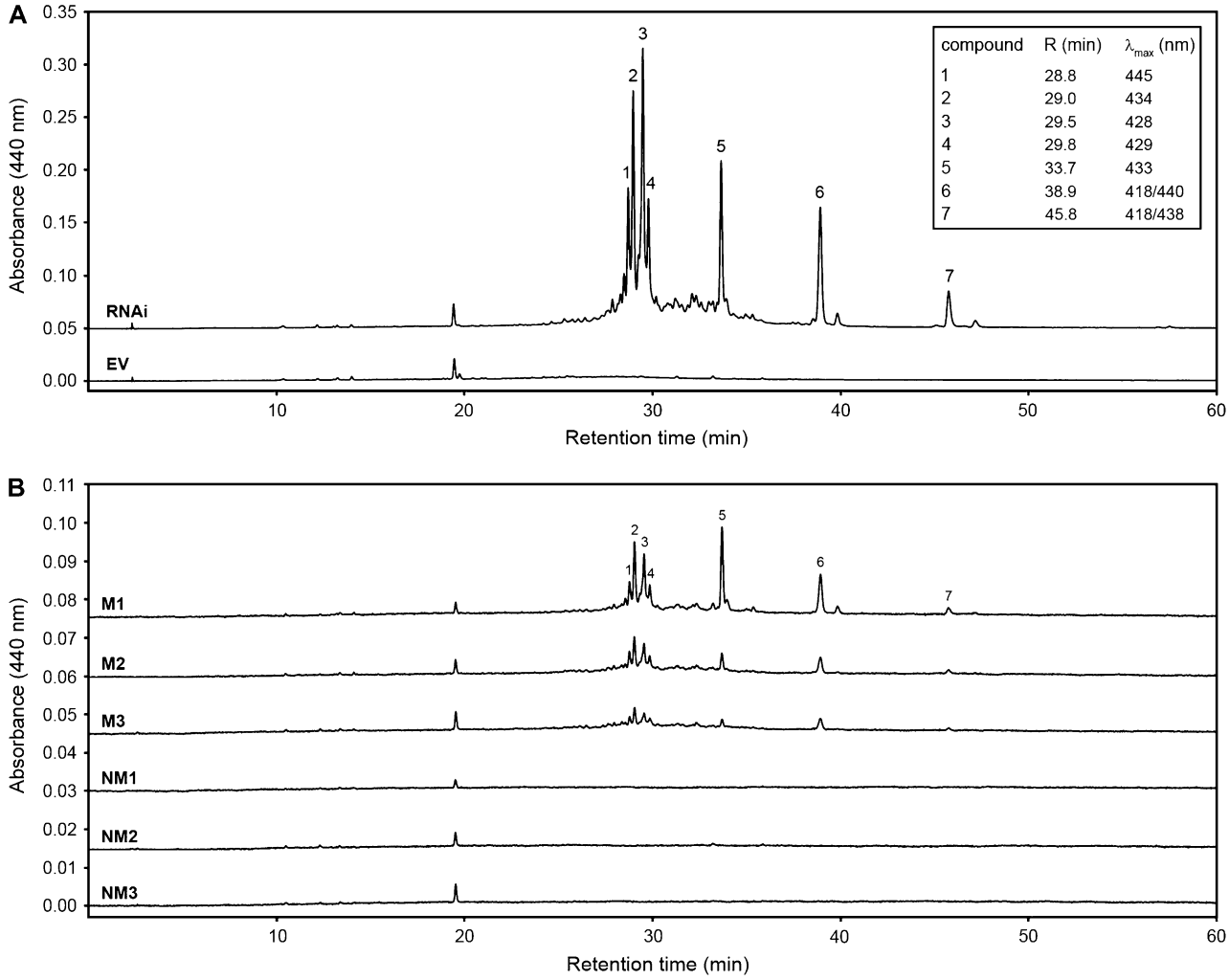

Figure 5. HPLC separation of methanolic extracts from hairy roots. A, Comparison of mycorrhizal EV control roots (bottom trace) and mycorrhizal RNAi roots (top trace) with compound detection at 440 nm. Separation of native constituents revealed seven novel compounds, which appear exclusively in RNAi samples. Corresponding UV absorption maxima are shown in the inset. B, Comparison between nonmycorrhizal (NM) and mycorrhizal (M) roots of three individual RNAi root systems each. Root extraction, separation conditions, and compound terminology were as in A.

of C_{40} carotenoids, which have absorption maxima at higher wavelengths.

Using our standard procedure for liberating mycorradicin from its derivatives (Floss et al., 2008), alkaline treatments of the extracts from the transgenic roots were performed. HPLC analyses revealed two major peaks, which exhibited UV light spectra with maxima at 428 and 434 nm, again reminiscent to C_{27} apocarotenoids (Fig. 6). The two compounds, with retention times of 19.1 and 21.8 min, respectively, termed Apo1 and Apo2, were isolated by semipreparative HPLC from methanolic root extracts after alkaline hydrolysis. To get data for their structures, the Apo1- and Apo2-containing fractions were subjected to liquid chromatography electrospray ionization mass spectrometry (LC-ESI/MS) analyses. Unfortunately, Apo1 coeluted with a compound showing a MS fragmentation pattern identical to that of the known root saponin bayogenin dihexoside (Huhman and Sumner, 2002; Huhman et al., 2005; Schliemann et al., 2008a), precluding identification. However, it was possible to identify Apo2. ESI-Fourier transformation ion cyclotron resonance (FTICR)-MS analysis indicated a $[M + H]^+$ ion with a mass-to-charge ratio (*m/z*) 733.37944 corresponding to $C_{39}H_{57}O_{13}$, compatible with a C_{27} 3-hydroxy-α-apo-10′-carotenoic acid glycosylated by two hexose moieties at the 3-hydroxyl position (Fig. 7). Due to the fact that AM-induced cyclohexenone derivatives characterized to date exclusively contain an α-ionone ring (Strack and Fester, 2006), this ionone type is also tentatively proposed for the C_{27} apocarotenoic acid identified. The 15-eV collision-induced dissociation (CID) mass spectrum of *m/z* 733 obtained from triple quadrupole MS shows a consecutive loss of

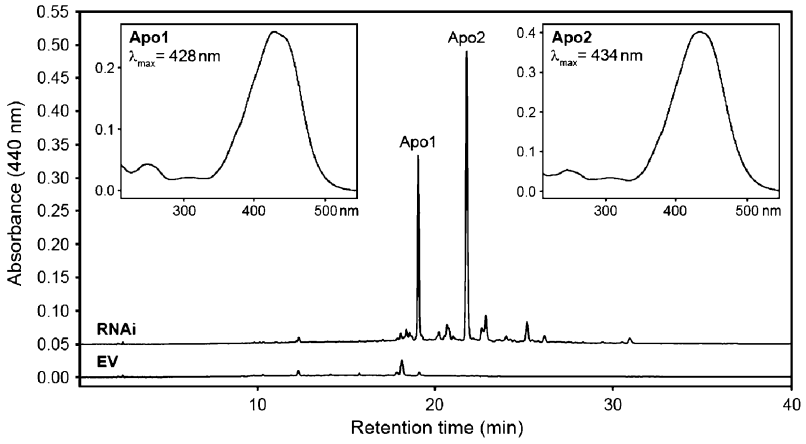

Figure 6. HPLC analysis of methanolic extracts from mycorrhizal hairy roots after alkaline hydrolysis. Comparison of EV and RNAi roots revealed two major compounds appearing in RNAi roots termed Apo1 and Apo2. Their UV light spectra and absorption maxima are shown in the insets. Separation and detection conditions were as described for Figure 5.

two hexose units (Δm = 162). The corresponding ions appear at *m/z* 571 $[M + H - 162]^+$ and *m/z* 409 $[M + H - 2 \times 162]^+$ (Fig. 7). A $[M + H]^+$ signal at *m/z* 409 and a UV light absorption maximum at 431.9 nm in 85% methanol/15% hexane has been reported for a C_{27} apocarotenoic acid aglycone (Cooper et al., 2003), which is almost identical with our data under our solvent conditions and provides evidence for the proposed aglycone structure (Fig. 7). A consecutive loss of two molecules of water from the hydroxy and carboxy groups may lead to *m/z* 391 (major peak) and *m/z* 373, respectively. Additional characterization of the aglycone was possible by the 25-eV ESI-CID mass spectrum. The ion at *m/z* 269 may result from splitting next to the ionone ring (a). Significant key ions at *m/z* 201 (b) and *m/z* 187 (c) may be formed by bond cleavages at the indicated positions. Based on these analyses, compound Apo2 has been tentatively identified as a C_{27} 3-hydroxy-α-apo-10′-carotenoic acid, glycosylated with two hexose moieties at the 3-hydroxyl position of the apocarotenoid (Fig. 7).

Root Colonization by AM Fungi and Transcript Levels of AM Molecular Markers Are Largely Unaltered upon *MtCCD1* Repression

Potential alterations in colonization by AM fungi of *MtCCD1*-silenced roots were analyzed by standard ink staining tests using the individual transgenic root systems of experiment I. Assessment and calculation of mycorrhizal colonization parameters were carried out according to Trouvelot et al. (1986). There were no significant changes in either the total colonization of roots (frequency of mycorrhizal structures; F%), the density of mycorrhizal structures (m%), or the abundance of ink-stainable arbuscules in the colonized part of the root (a%; Fig. 8, A–C). A slight upward trend for F% and a% was recognizable rather than an adverse effect, but whether this is a reproducible effect requires further experiments.

Arbuscules are ephemeral structures that constantly decay and reemerge with a life span of 7 to 10 d (Alexander et al., 1988). Following up earlier assessments of the ratios of various stages of arbuscule development in arbuscule populations (Floss et al., 2008), an acid-fuchsin staining analysis was performed. Confocal images of arbuscules from these stainings were used to classify individual arbuscules into four developmental stages ranging from early development to fully degraded and dead arbuscules, as described (Floss et al., 2008). The most obvious alteration in *MtCCD1*-repressed roots was a moderate, yet significant, increase in degenerating arbuscules from 32% to 48% of the total population of arbuscules (Fig. 8D).

In addition, the transcript levels of several AM molecular marker plant genes were determined by real-time reverse transcription (RT)-PCR. These markers include *MtDXS2-1* as an AM-inducible gene involved in early steps of apocarotenoid biosynthesis (Walter et al., 2002; Floss et al., 2008) and *MtPT4* as an AM-specific phosphate transporter (Harrison et al., 2002; Table I). Other AM markers have been specified by transcriptome analyses of mycorrhizal roots (Hohnjec et al., 2005) and have been used previously to assess alterations in mycorrhizal physiology upon *MtDXS2* repression (Floss et al., 2008). None of the AM plant markers used in this study showed significant alterations in their transcript levels in mycorrhizal RNAi roots relative to mycorrhizal EV controls (Table II). The only exception exhibiting a minor, yet significant, decrease was *MtLEC7*, an AM-inducible lectin gene (Frenzel et al., 2005). Taken together, there was no indication of a major impairment of the AM symbiosis by silencing *MtCCD1* expression.

DISCUSSION

In our studies on apocarotenoid biosynthesis, an experimental system of a symbiotic plant-microbe interaction (AM) is employed, which has turned out to be very useful (Walter et al., 2002; Hans et al., 2004; Floss et al., 2008). First, apocarotenoid biosynthesis in roots is inducible upon colonization by AM fungi and leads to massive accumulation of apocarotenoids. This proceeds in an apparently cell-specific manner related

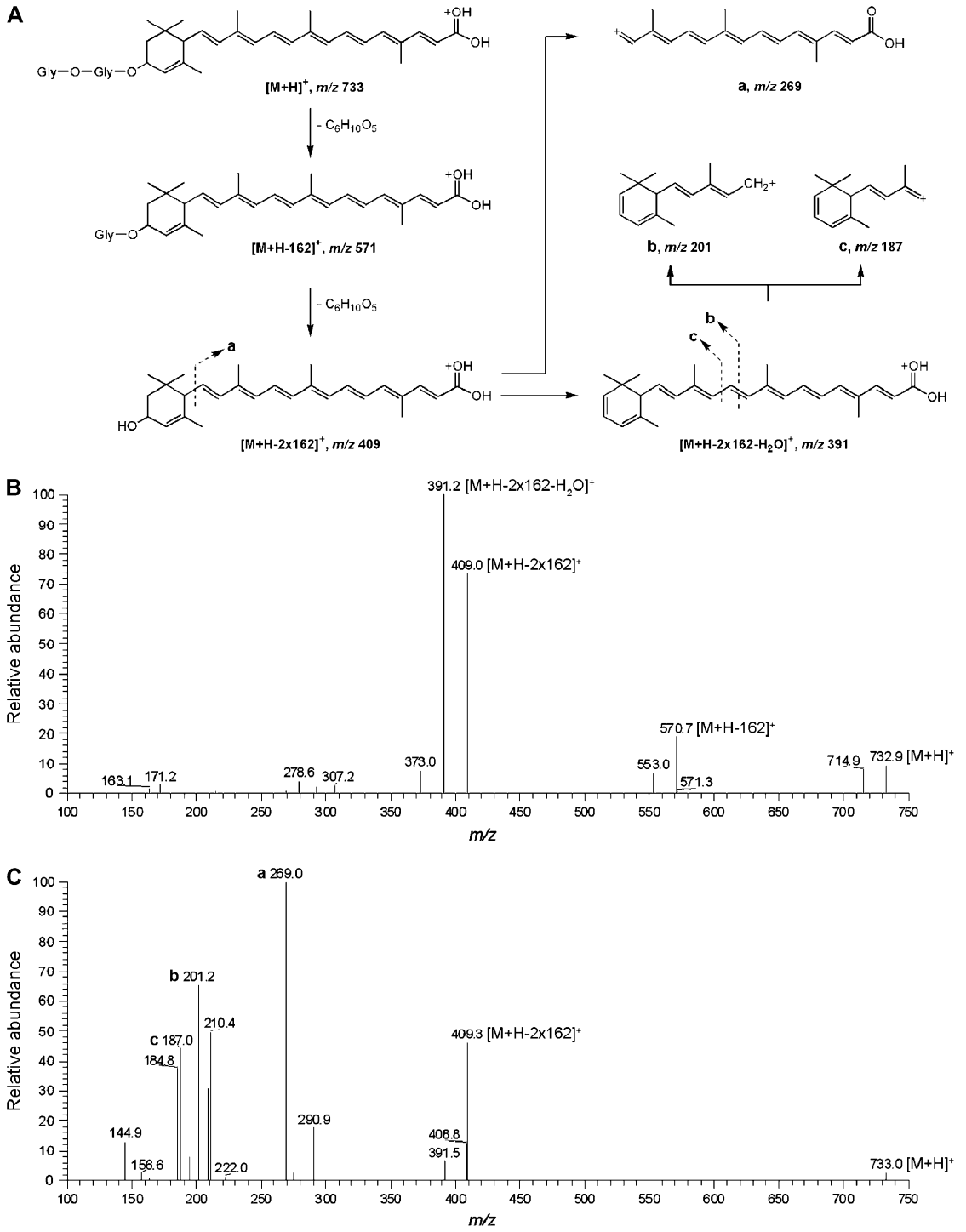

Figure 7. Mass spectral analysis of compound Apo2. A, Scheme of the proposed fragmentation of compound Apo2, whose proposed structure is shown at top left. Apo2 exhibits a *m/z* of 733 $[M + H]^+$. Removing one or two hexose residues (increments of 162) results in fragments with *m/z* 571 and 409. Splitting of the aglycone next to the cyclohexene ring is proposed to yield fragment a (*m/z* 269). Additional fragments may be derived from fragmentation in the linear side chain of the Apo2 aglycone (*m/z* 391) at the positions indicated, resulting in fragments of *m/z* 201 (b) or *m/z* 187 (c). B and C, ESI-CID mass spectra of Apo2 (B, 15 eV; C, 25 eV).

to the occurrence of fungal arbuscules (Fester et al., 2002a; Floss et al., 2008). Second, this accumulation involves transcriptional up-regulation of various steps of carotenoid biosynthesis and cleavage (Walter et al., 2000, 2002; Fester et al., 2002b; Hans et al., 2004; Sun et al., 2008; Table I). Third and most important for this

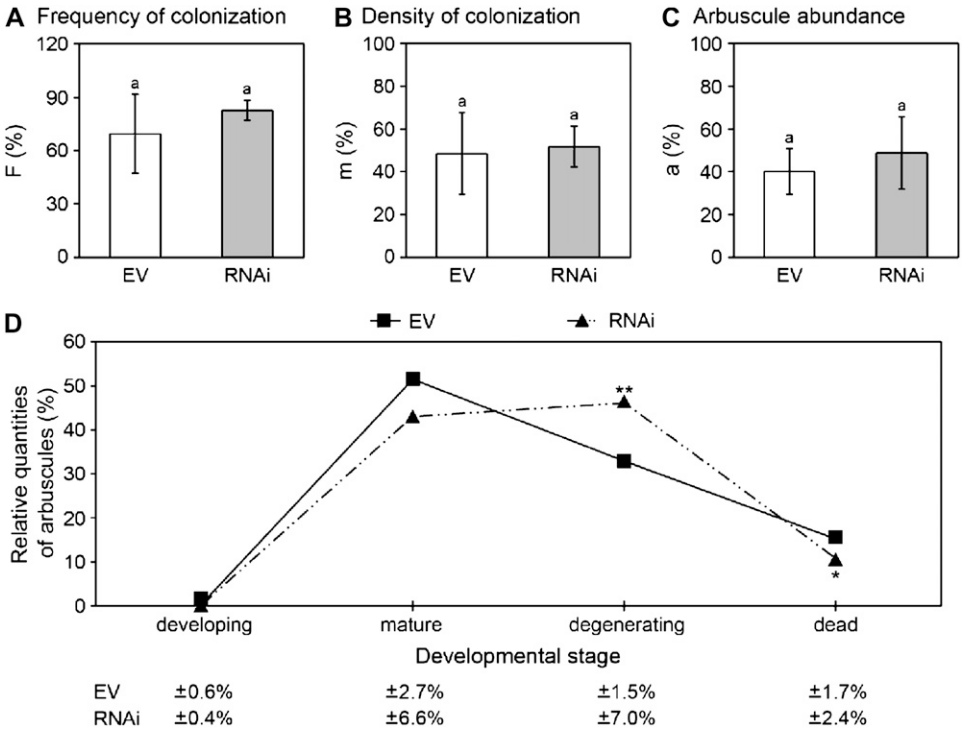

Figure 8. Assessment of mycorrhizal parameters from stained mycorrhizal roots of EV controls and RNAi plants of experiment I. A to C, Ink-staining analyses conducted and evaluated according to Trouvelot et al. (1986) using eight samples each of EV controls and RNAi roots. A, Frequency of fungal structures (F%). B, Density of fungal structures in the mycorrhizal part of the root (m%). C, Arbuscule abundance in the mycorrhizal part of the roots (a%). D, Evaluation of arbuscule morphologies from confocal images after acid-fuchsin staining of roots. Individual arbuscules were classified into one of four developmental stages as indicated using four samples each of EV controls and RNAi roots (containing 3%–6% residual *MtCCD1* transcripts). One hundred arbuscules were evaluated from each root system. Statistical significance of alterations was analyzed by the Kruskal-Wallis test (developing stage) or the one-way test (other stages). * $P \leq 0.05$; ** $P \leq 0.01$. SD values are shown below the graph.

study, the metabolic fate of primary carotenoid cleavage products is different from that in other systems. In the mycorrhizal root system used here, both the C_{13} and C_{14} cleavage products are easily traceable as oxidized and further modified downstream metabolites. In particular, the central C_{14} linear product of C_{40} carotenoid cleavage is converted to a stable yellow dicarboxylic acid (mycorradicin) usually accumulating in esterified form (Fester et al., 2002a). The ratio of C_{13} to C_{14} apocarotenoid end products in mycorrhizal roots exhibits large variations ranging from 0.4 to 0.5 in the system used here (Fig. 3) through values of 1 to 2 in AM wild-type roots of *M. truncatula* or in AM cereal roots (Walter et al., 2000; Schliemann et al., 2008a) to as high as 27 in AM *Allium porrum* roots (Schliemann et al., 2008b). These fluctuations argue for a variable metabolic fate of apocarotenoids in mycorrhizal roots of individual plant species. In other nonmycorrhizal systems, the C_{14} primary cleavage product often escapes detection, since it is further metabolized to unknown products or is not volatile enough for gas chromatography-MS analysis (Auldridge et al., 2006a; Ibdah et al., 2006; Sun et al., 2008). One alternative system, in which the fate of the C_{14} product has been investigated to some extent, is the rose petal, where a reduced C_{14} dialdehyde downstream product has been identified: the diol rosafluene. This dialcohol has been characterized as being colorless and unstable (Eugster and Märki-Fischer, 1991), as opposed to the oxidized C_{14} metabolite mycorradicin and its derivatives.

In this system of easy traceability of all predicted carotenoid cleavage products, we could clearly recognize a differential reduction of C_{13} and C_{14} metabolites upon knockdown of *MtCCD1* expression in mycorrhizal hairy roots of *M. truncatula*. The C_{14} cleavage products (mycorradicin derivatives) were strongly reduced almost to the limits of detection upon strong repression of *MtCCD1*, whereas the C_{13} cleavage products (cyclohexenone derivatives) were only reduced to about 30% to 50% of the levels of EV controls (Fig. 3). This suggests that mycorradicin biogenesis depends on MtCCD1 activity but also that only one of the two C_{13} cleavage products expected from the presumed symmetrical cleavage of C_{40} carotenoid precursors (Fig. 1) originates from this activity. The other one appears to be generated by the action of a different enzyme. The results obtained from two extensive experiments of *MtCCD1* silencing with many biological replicates are clearly contradictory to the hitherto discussed scheme of CCD1 action (Fig. 1).

Table II. *Transcript levels of AM molecular marker plant genes in mycorrhizal hairy roots harboring the EV vector or the MtCCD1 RNAi construct determined from samples of experiment I*

A single significant alteration is indicated in boldface. Four biological replicates were assayed in each case by real time RT-PCR.

DFCI Identifier	Gene	$E^{\Delta Ct} \times 10^{-3}$	
		EV	RNAi
TC94453	*MtPT4*	146.5 ± 49.2	124.2 ± 56.6
TC95018	*MtGLP1*	169.3 ± 41.2	170.6 ± 72.6
TC95567	*MtLEC7*	**80.3 ± 19.7**	**42.8 ± 7.4**
TC95651	*MtDXS2-1*	12.2 ± 3.0	10.8 ± 4.7
TC96500	*MtBCP1*	5.0 ± 1.2	3.9 ± 1.7
TC100720	*MtGST1*	96.3 ± 21.6	76.9 ± 19.3
TC106954	*MtSCP1*	22.0 ± 5.0	18.2 ± 4.6

Concomitant with the differential reduction of C_{13} and C_{14} apocarotenoids, a conspicuous color change was observed as a consequence of *MtCCD1* repression. The rather faint orange-brown coloration of mycorrhizal EV control roots related to mycorradicin derivative accumulation was modified to a clearly more intense yellow-orange root color, indicating the accumulation of a different abundant chromophore (Fig. 4). This coloration also differed from the bright yellow color frequently observed in many cereal roots after mycorrhization, indicating massive accumulation of mycorradicin derivatives (Klingner et al., 1995; Walter et al., 2000). Root extraction and analysis by HPLC revealed the emergence of at least seven novel compounds in mycorrhizal RNAi roots (Fig. 5). Their UV spectra were similar to those of C_{27} apocarotenoid structural variants recently reported with single absorption maxima between 428 and 440 nm (Cooper et al., 2003). In particular, these spectra matched most closely to several C_{27} carboxylic acids reported by those authors. There was no indication of an accumulation of C_{40} carotenoids, which had been expected at the outset of our studies based on the previous hypothesis of CCD1 action (Fig. 1).

The methanolic extracts of RNAi roots were subjected to alkaline hydrolysis, resulting in only two major compounds again exhibiting characteristics of C_{27} apocarotenoids (Fig. 6). Based on ESI-MS and MS/MS, the structure of Apo2 was proposed to be a C_{27} carboxylic acid (3-hydroxy-α-apo-10′-carotenoic acid) linked with two hexose moieties at the 3-hydroxy position of the cyclohexene ring (Fig. 7). At least three key fragments (*m/z* 409, 391, and 269) conform precisely to major fragments obtained earlier by atmospheric pressure chemical ionization MS and MS/MS from a nonglycosylated 3-hydroxy-β-apo-10′-carotenoic acid (Cooper et al., 2003), corroborating the proposed structure. While there is still ambiguity on the position of the double bond in the cyclohexene ring (β- or α-ionone type), the α-ionone (ε-ring) type appears to be more likely. It has always been found in structural analyses of C_{13} cyclohexenone derivatives obtained from mycorrhizal roots (Strack and Fester, 2006; Walter et al., 2007). In addition, there is no explanation yet for the origin of the keto group in these derivatives. Therefore, the tentatively proposed but still unknown precursor for the AM-induced apocarotenoids is likely to be neither zeaxanthin (β,β-carotene rings) nor lutein (β,ε-rings). Whether the less common xanthophyll lactucaxanthin (Cunningham and Gantt, 2001) derived from ε,ε-carotene containing two α-ionone-like rings (ε-rings) is involved in this pathway is currently a rather speculative assumption. The C_{27} 3-hydroxy-α-apo-10′-carotenoic acid is an intermediate predicted to be formed analogous to mycorradicin by a single instead of a double cleavage of this proposed xanthophyll precursor. The 3-hydroxy position of the C_{27} compound was found to be glycosylated in the extracts from RNAi roots, as opposed to the C_{13} cyclohexenone derivatives containing a keto group, indicating that its conversion into the keto group in the cyclohexene moiety may not be possible with the C_{27} apocarotenoid intermediate. MtCCD1 thus appears to catalyze the $C_{27} \rightarrow C_{14} + C_{13}$ cleavage but not the $C_{40} \rightarrow C_{27} + C_{13}$ cleavage. Taken together, there is ample evidence for the accumulation of several C_{27} apocarotenoids, most probably differently esterified, in mycorrhizal roots caused by silencing of *MtCCD1* expression. C_{27} apocarotenoids have never been observed in wild-type mycorrhizal roots. Derivatives of C_{27} apocarotenoid core structures have only occasionally been identified in plants, perhaps due to the abundant activities of CCD1 enzymes in many plant tissues (Simkin et al., 2004b; Auldridge et al., 2006a). Examples for natural C_{27} apocarotenoid occurrence, either as carboxylic acids or as alcohols, are flowers of *Boronia megastigma* (Cooper et al., 2003), rose petals (Eugster and Märki-Fischer, 1991), and roots of *Escobedia scabrifolia* (azafrin; Kuhn and Brockmann, 1935).

The emergence of C_{27} apocarotenoids and not, as expected, C_{40} carotenoids upon blocking *MtCCD1* gene expression in mycorrhizal RNAi roots clearly suggests the C_{27} apocarotenoids as the substrates of the MtCCD1 enzyme in planta. It further suggests a consecutive two-step cleavage mechanism of carotenoids following the schemes $C_{40} \rightarrow C_{27} + C_{13}$ and $C_{27} \rightarrow C_{14} + C_{13}$. Such a mechanism was proposed a number of years ago (Eugster and Märki-Fischer, 1991), but this scheme was abandoned in the wake of many studies on recombinant CCD1 proteins in *E. coli* showing symmetrical cleavage of a wide variety of C_{40} carotenoids in vitro. However, the in planta substrate(s) of the enzyme has remained elusive. Interestingly, a recent study on an Arabidopsis CCD1 loss-of-function mutant (*ccd1-1*) also came up with surprisingly few, if any, changes in precursor C_{40} carotenoid accumulation in the mutant. Leaf carotenoid levels were completely unchanged. Total seed carotenoid levels were significantly elevated by about 30% (Auldridge et al., 2006a). While this appears to indicate that CCD1 acts on C_{40} carotenoids at least in seeds, the result could also be explained by a feedback mechanism down-regulating

the first cleavage step ($C_{40} \rightarrow C_{27} + C_{13}$) upon abnormal accumulation of the C_{27} apocarotenoid intermediate, resulting from failure of the second step ($C_{27} \rightarrow C_{14} + C_{13}$; CCD1). A potential accumulation of C_{27} apocarotenoids in the *ccd1-1* mutant was not investigated, and a phenotype was not observed. Moreover, in an antisense approach on *CCD1* expression in tomato, two transgenic lines with more than 90% reduction in *CCD1* transcript levels were obtained, yet the reduction in C_{13} apocarotenoid volatile emission was only about 50% (Simkin et al., 2004a), reminiscent of the cyclohexenone derivative contents obtained in our study (Fig. 3). Fruit carotenoid content was not affected in these antisense plants. The authors concluded the likely existence of redundant activities for C_{40} carotenoid cleavage (Simkin et al., 2004a). Similarly, strong cosuppression of *PhCCD1* led to unexpectedly high residual levels of 24% to 42% in C_{13} β-ionone emission from petunia (*Petunia hybrida*) flowers (Simkin et al., 2004b). The conclusion of these authors for additional players in C_{40} carotenoid cleavage is supported by our data, but with the crucial difference that this is likely not a redundant but a complementary activity of at least two players in a cleavage process of C_{40} to C_{14} and C_{13} compounds in two consecutive steps. The results obtained with the mycorrhizal root system, therefore, may be of general importance for the mechanisms of carotenoid cleavage in planta. Further supportive evidence comes from an in vitro study on recombinant AtCCD1 showing C_{13} β-ionone formation using a C_{30} apocarotenoid as substrate (Schmidt et al., 2006). Moreover, recent studies in the cyanobacterium *Nostoc* sp. PCC 7120 demonstrated the preference of a recombinant NosCCD (identical to previous NSC1) for cyanobacterial monocyclic C_{40} xanthophyll substrates compared with bicyclic xanthophylls like zeaxanthin or canthaxanthin (Marasco et al., 2006; Scherzinger and Al-Babili, 2008). The NosCCD, structurally related to plant CCD1, also exhibits strong apocarotenal cleavage activity for both C_{30} 3-hydroxy-β-apo-8′-carotenal and C_{27} 3-hydroxy-β-apo-10′-carotenal (Scherzinger and Al-Babili, 2008). These findings corroborate the notion that the major substrates for CCD1 enzymes in planta may not be C_{40} carotenoids but rather C_{27} apocarotenoid compounds.

The new view on carotenoid cleavage in planta brought forward here and summarized in Figure 9 may also reconcile a long-standing contradiction of how CCD1 enzymes get access to their substrates. CCD1 enzymes have been shown in several experimental systems and by several criteria to be located in the cytosol (Bouvier et al., 2003; Tan et al., 2003; Simkin et al., 2004a; Auldridge et al., 2006a). So how should CCD1 get access to their presumed C_{40} carotenoid substrates located within the plastid and separated from the CCD1 location by the plastidial membrane? The solution may be that in vivo C_{40} is a substrate for CCD1 only after damage or breakdown of plastids and release of C_{40} carotenoids into the cytosol. In intact plastids, CCD1 probably never gets access to C_{40} carotenoids. The primary $C_{40} \rightarrow C_{27} + C_{13}$ conversion is thus likely to take place inside the plastid, after which these two apocarotenoids are exported from the plastid to the cytosol by unknown mechanisms. Once in the cytosol, the C_{27} apocarotenoid can be further cleaved by abundant cytosolic CCD1 to a second C_{13} molecule and a C_{14} molecule. An export of C_{27} compounds into the cytosol is suggested by the finding that a glycosylated form of the C_{27} apocarotenoid carboxylic acid has been isolated (Fig. 7). Glycosylation is a common modification carried out by cytosolic glycosyltransferases. In ABA biosynthesis, the primary carotenoid cleavage of C_{40} cis-carotenoids catalyzed by NCEDs occurs inside the plastid in an analogous manner to that now proposed for C_{13} and C_{14} apocarotenoid biosynthesis. The C_{15} aldehyde ABA precursor (xanthoxin) then leaves the plastid through unknown mechanisms, and subsequent modification steps are extraplastidial (Nambara and Marion-Poll, 2005). Taken together, our new model for the in planta cleavage of C_{40} carotenoids to C_{14} and C_{13} products organized in two consecutive steps in different cellular compartments (Fig. 9) is compatible with the data obtained in this study and with those from other laboratories.

What then could be the elusive CCD enzyme to perform the first cleavage step and generate C_{27} from C_{40} inside the plastid? One certainly cannot fully exclude the existence of an unknown novel CCD, but this CCD should then be completely unrelated in amino acid sequence to the existing nine CCD classes. This is considered rather unlikely. From the known CCDs, a prime candidate is CCD7, with the required 9,10 double bond cleavage specificity and a reported plastidial location. So far, only recombinant AtCCD7 has been shown to cleave C_{40} to C_{27} in *E. coli* (Schwartz et al., 2004). Native CCD7 (MAX3) is involved in one of two consecutive cleavage reactions necessary for the generation of a novel carotenoid-derived hormone. This hormone acting as an inhibitor of shoot branching is generated by the genes of the *max* pathway of Arabidopsis and by orthologous genes in many other plants, exemplified by *rms5* in pea (*Pisum sativum*) and *htd1* in rice (*Oryza sativa*; Booker et al., 2004, 2005; Snowden et al., 2005; Johnson et al., 2006; Zou et al., 2006; Mouchel and Leyser, 2007). The second cleavage activity required for the biosynthesis of the branching inhibitor is contributed by CCD8. Schwartz et al. (2004) showed cleavage activity of a recombinant AtCCD8 on a C_{27} substrate, resulting in C_{18} and C_9 cleavage products. On the other hand, Auldridge et al. (2006a) reported cleavage of C_{40} carotenoid substrates to unknown products by recombinant AtCCD8.

More recently, the strict specificity of CCD8 for certain C_{27} compounds (β-apo-10′-carotenal and its alcohol), the conservation of this specificity in monocot and dicot species, and the nature of the C_{18} product (β-apo-13-carotenone) have been further elucidated (Alder et al., 2008). AtCCD7, however, cleaves multi-

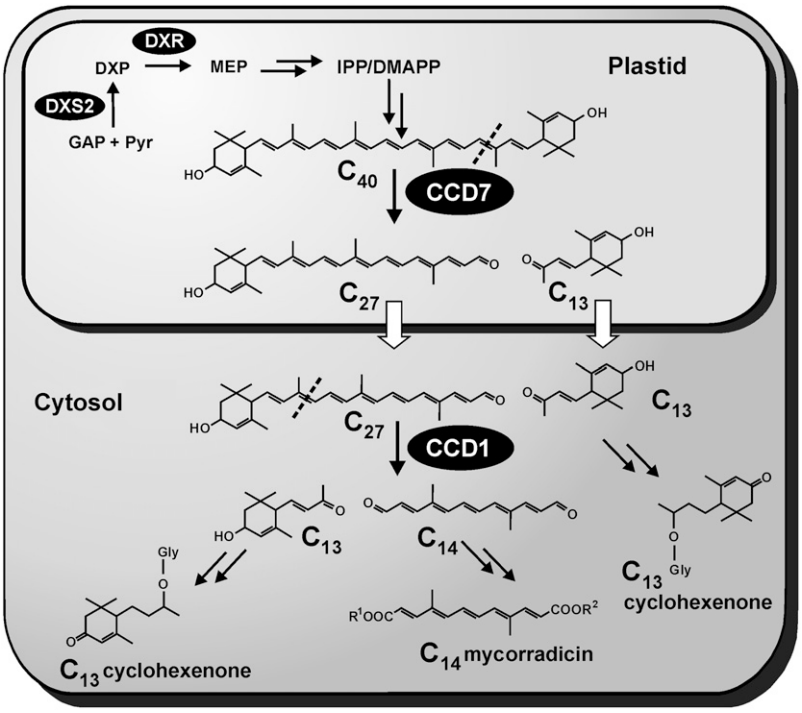

Figure 9. Proposed organization of C_{40} carotenoid formation and cleavage to apocarotenoids in a compartmentalized mycorrhizal root cell. C_{40} carotenoids (exemplified by lactucaxanthin as the tentatively proposed precursor for AM-induced apocarotenoids) synthesized inside plastids are proposed to be cleaved by plastidial CCD7 to one C_{27} aldehyde and one C_{13} ketone intermediate, which both can be exported into the cytosol in an unmodified or modified state (white arrows). The C_{27} intermediate in the cytosol is further cleaved by CCD1 to a C_{14} and a second molecule of C_{13}, which are, together with the first C_{13} molecule, modified to yield the oxidized C_{13} and C_{14} apocarotenoids (cyclohexenone and mycorradicin derivatives) found in mycorrhizal roots. For abbreviations, see Figure 1.

ple C_{40} carotenoids, including lycopene, β-carotene, and zeaxanthin (Booker et al., 2004), leading to the prospect that its biological function is not limited to the formation of the branching inhibitor (Alder et al., 2008). In addition, while double mutants of Arabidopsis *ccd7* (*max3-11*) and *ccd8* (*max4-6*) were phenotypically indistinguishable from either single mutant, a quantitative dosage effect of *ccd8* heterozygotes on the branching phenotype argues for CCD8 activity as a limiting step in the pathway (Auldridge et al., 2006a). The reported strict specificity of CCD8 for the conversion of C_{27} β-apo-10′-carotenal and its inability to convert 3-hydroxy-β-apo-10′-carotenal (Alder et al., 2008) appear to preclude a common C_{27} precursor for both the branching inhibitor and mycorrhizal apocarotenoids. In support of this preliminary conclusion, we have never observed an obvious branching phenotype on strongly mycorrhized plants, which might possibly arise from depleted C_{27} common precursor pools. The data available at present are thus in agreement with CCD8 catalyzing a specific step in a side route from C_{27} to the branching inhibitor, while CCD7 might be required for both branching inhibitor and mycorrhizal apocarotenoid biosynthesis (Fig. 9). Finally, while this article was under revision, two reports became available online, suggesting strigolactones as the long sought after carotenoid-derived branching inhibitor hormone and confirming the specific role of CCD8 in its synthesis (Gomez-Roldan et al., 2008; Umehara et al., 2008).

Based on other very recent data, CCD4 must now also be considered a potential player for the in planta generation of C_{27} apocarotenoids. Earlier investigations have attributed 7,8 (7′,8′) cleavage activity to a CsZCD of saffron, representing an incomplete CsCCD4 sequence (Bouvier et al., 2003), but the aforementioned recent work now reports β-ionone formation from recombinant full-length CsCCD4 acting on β-carotene as a substrate in *E. coli*, which implies 9,10 and/or 9,10 (9′,10′) cleavage activity (Rubio et al., 2008). CCD4 also fulfills the condition of having a proven localization within plastids in plastoglobules (Ytterberg et al., 2006), but it has not been shown to produce C_{27} apocarotenoids in vitro. As for the in planta action of CCD4, an RNAi-silencing approach on *CCD4* expression in white-petal cultivars of *Chrysanthemum morifolium* resulted in the generation of yellow petals, which indicates that the white-petal phenotype is brought about by carotenoid degradation (Ohmiya et al., 2006). Loss of function of *CCD4* thus strongly increased carotenoid content in *Chrysanthemum* petals as opposed to no or minor effects upon silencing or mutating *CCD1* genes (Simkin et al., 2004a, 2004b; Auldridge et al., 2006a).

While one cannot make a safe case for either CCD7 or CCD4 as the missing player for the $C_{40} \rightarrow C_{27}$ cleavage at this time, there are a couple of arguments favoring CCD7 at least for the mycorrhizal apocarotenoids. Mining of the extensive *M. truncatula* EST databases does not indicate the presence of *MtCCD4*-related transcripts in roots or mycorrhizal roots, whereas 18 ESTs can be identified from leaf, stem, and pod libraries. Lack of root expression and strong expression in flower or reproductive tissues has also been reported for *Chrysanthemum* and saffron *CCD4* genes (Ohmiya et al., 2006; Rubio et al., 2008). On the contrary, *CCD7* and *CCD8* are preferentially expressed in roots (Booker et al., 2004; Snowden et al., 2005; Auldridge

et al. 2006a). Preliminary analyses in our laboratory of transcript levels of *CCD7*-like sequences by RT-PCR in nonmycorrhizal and mycorrhizal roots of *M. truncatula* also demonstrated their fairly abundant presence in these tissues. Furthermore, preliminary supportive evidence for a role of CCD7 in mycorrhizal roots is now available from an analysis of mycorrhizal *rms5* (*CCD7*) mutant plants of pea (for their origin, see Johnson et al., 2006), which exhibited strongly reduced levels of C_{13} cyclohexenone and C_{14} mycorradicin derivatives compared with mycorrhizal wild-type plants (M.H. Walter, unpublished data).

Besides clarifying the role of CCD1 in the biosynthesis of cyclohexenone and mycorradicin derivatives, our RNAi approach was also meant to elucidate potential functions of either of these apocarotenoids in the AM symbiosis. Such functions might be revealed by the reduction or lack of these compounds in roots of RNAi plants. To proceed toward this goal, we determined the transcript levels of several AM molecular markers. However, neither *MtPT4* nor any of the other markers showed a strong decrease (Table II) comparable to the strong down-regulation recently obtained by strong silencing of *MtDXS2* (Floss et al., 2008). Then again, the differential reduction of cyclohexenone and mycorradicin derivatives constitutes an opportunity to enter into a discussion on which of the two apocarotenoids might be a major player in the AM symbiosis. Despite strong reduction of mycorradicin derivative levels in *MtCCD1* RNAi roots (Fig. 3), the AM molecular markers were largely unaltered (Table II), arguing against a contribution of mycorradicin to the effect on these markers. On the contrary, cyclohexenone derivative levels were reduced to only 30% to 50% of those of EV controls (Fig. 3), which might simply not be sufficient to strongly affect AM marker gene expression. Extensive reduction of cyclohexenone derivative levels as accomplished by strong *MtDXS2* silencing reproducibly led to a dramatic abolishment of AM-induced plant marker gene expression (Floss et al., 2008). In the *MtCCD1*-silenced roots used here, one of the AM markers (*MtLEC7*) exhibited a minor, but significant, down-regulation (Table II). Interestingly, this marker was also negatively affected in roots moderately silenced for *MtDXS2* expression, while all other markers were unaltered (Floss et al., 2008). The outcome of strong repression of *MtCCD1* thus appears to be similar to the moderate repression of *MtDXS2*, which both share moderately but not strongly reduced levels of cyclohexenone derivatives (Table II; Floss et al., 2008).

While any consequences of the strong silencing of *MtCCD1* on AM molecular markers were hardly detectable, a commonality to *MtDXS2* silencing was the significant increase in older, degenerating arbuscules (Fig. 8D; Floss et al., 2008). Again, these alterations follow quantitatively the moderate alterations of cyclohexenone derivatives in *MtCCD1*-silenced roots more closely than the strongly decreased levels of mycorradicin derivatives. Only a further reduction of cyclohexenone derivatives, as achieved in the *MtDXS2*-silencing approach, led to a more pronounced effect on the numbers of degenerating arbuscules and added an increase in dead arbuscules (Floss et al., 2008). Additional experiments recently indicated that with the *MtDXS2* target, moderate levels of silencing and cyclohexenone derivative reduction can also bring about an increase in the number of degenerating arbuscules independent of the strong drop in AM marker transcript levels (D.S. Floss and M.H. Walter, unpublished data). These results lend further support to a possible link between the moderate reduction of cyclohexenone derivative levels (Fig. 3) and the moderate increase in arbuscules at the degenerating stage (Fig. 8D). Both of the observations of changes of AM marker transcript levels and of the number of degenerating arbuscules are thus compatible with a role of cyclohexenones in these two instances, which is in agreement with previous arguments (Walter et al., 2007). Mycorradicin derivatives accumulate massively next to degenerating arbuscules within osmiophilic droplets finally located to vacuoles (Fester et al., 2002a). These derivatives might have other functions in the decay and reemergence of arbuscules, but they seem to be not directly involved in regulating the number of physiologically active arbuscules.

CONCLUSION

While the definite roles of cyclohexenone and mycorradicin derivatives in the AM symbiosis still need to be clarified, this report sheds new light on the mechanism of carotenoid cleavage and on its compartmentation in plant cells. It is now most interesting to search for C_{27} apocarotenoids accumulating in other *CCD1*-repressed plants or respective mutants. Moreover, a potential contribution of CCD7 and/or CCD4 to the generation of flower scents, fruit aromas, or the flavor of wines complementing CCD1 activities (Simkin et al., 2004a; Mathieu et al., 2005) will now be a promising area to study. For mycorrhizal research, the *CCD7* gene will constitute a new target to modify the levels of mycorrhizal apocarotenoids and to finally elucidate their function in the AM symbiosis.

MATERIALS AND METHODS

Plant Cultivation and Fungal Inoculation

Medicago truncatula var. Jemalong was cultivated in pots on expanded clay substrate (Lecaton; Fibo Exclay) in a greenhouse during the months of June and July (RNAi experiments) or December and January (wild-type cultivation) with a 16-h daily light period. Plants were supplied with deionized water three times per week and with a phosphate-reduced fertilizer (10 mL of half-strength Long Ashton medium, 20% of regular phosphate) once a week. Seven-day-old wild-type plantlets or 6-week old plants from hairy root transformation with transgenic root systems and wild-type shoots were inoculated with the AM fungus *Glomus intraradices* isolate 49 provided by H. von Alten (University of Hannover; Maier et al., 1995). This was done by transferring to clay substrate containing 30% (v/v) fungal inoculum enriched

in propagules by previous cocultivation with *Allium porrum* 'Elefant' as described (Floss et al., 2008).

MtCCD1 cDNA Cloning and Expression in *Escherichia coli*

An 825-bp fragment of a *MtCCD1* cDNA was amplified from mycorrhizal root RNA of *M. truncatula* using the primers MtCCD1c-fw (5′-AGCTGTTGATTTATTGGAGAAG-3′) and MtCCD1c-re (5′-ATCAGTGTCTTATTCTTCACC-3′) deduced from TC100912 of the DFCI *M. truncatula* gene index (version 8; http://compbio.dfci.harvard.edu/tgi/cgi-bin/tgi/gimain.pl?gudb=medicago). This fragment was used as a probe to screen a cDNA library from *M. truncatula* mycorrhizal roots as described (Walter et al., 2002). Several full-length clones with sequence identity to TC100912 were obtained.

For bacterial expression, the coding sequence of *MtCCD1* was amplified from the cDNA using the primers MtCCD1ex-fw (5′-TATCCATGGAGTCTGAGAAAATAGGAGG-3′) and MtCCD1ex-re (5′-TATCTCGAGCAGTTTAGCTTGTTCTTG-3′) and cloned in the *Nco*I and *Xho*I sites of the expression vector pET-28a(+). A second construct including a C-terminal His tag was generated using the same MtCCD1ex-fw primer but the reverse primer MtCCD1ex-His-re (5′-TATCTCGAGTTACAGTTTAGCTTGTTCTTG-3′). Expression was done in *E. coli* strain BL21(D3) containing either the pAC-BETA or the pAC-ZEAX plasmid (Cunningham et al., 1996; Sun et al., 1996). Transformation was also done with pET-28(+) as an EV control. The various *E. coli* strains raised in suspension cultures were streaked on agar plates containing 50 mg mL^{-1} ampicillin and 0.1 mM isopropyl β-D-1-thiogalactopyranoside to reveal decoloration of carotenoids through recombinant MtCCD1 activity.

Generation of the RNAi Construct and Hairy Root Transformation

To generate an MtCCD1-RNAi construct, a 335-bp region covering 229 bp of 3′ coding and 106 bp of 3′ untranslated sequences was amplified from the cDNA by primers MtCCD1-RNAi-fw (5′-TATACTAGTGGCGCGCCTCTGAGGCTGTTTATGTTCC-3′) and MtCCD-RNAi-re (5′-TATGGATCCATTTAAATCTCTACTGCATTGTAGAATATCC-3′) and cloned into the *Spe*I-*Asc*I and *Bam*HI-*Swa*I sites of the pRNAi vector carrying DsRED1 as a fluorescent marker (Limpens et al., 2004). Details of the cloning process and further steps of construct introduction into *Agrobacterium rhizogenes* ArquaI as well as the hairy root transformation procedure have been described (Floss et al., 2008). Briefly, 7-d-old *M. truncatula* seedlings were injected with small volumes of bacterial culture (50–100 μL) three to five times into their hypocotyls. Seedlings were transferred into humid expanded clay for a 2-d recovery and then placed in a growth chamber (20°C, 16 h of light/8 h of dark) for 2 weeks, after which emerging hairy roots were covered by a vermiculite:sand (1:1) mixture. Four weeks after *A. rhizogenes* injection, a first screen for DsRED1 fluorescent roots was performed with a fluorescence stereomicroscope (Leica MZ FLIII with a DsRED1 filter), removing from each plant individually all nonfluorescent hairy roots as well as the wild-type roots. A second screen was carried out after a further 2 weeks of cultivation. Composite plants carrying exclusively transgenic roots were then inoculated with *G. intraradices* and further cultivated as described above.

Metabolite Analyses

Homogenized root samples (200 mg) from individual plants were each extracted three times with 400 μL of 80% aqueous methanol. After centrifugation, the supernatants were analyzed by reverse-phase HPLC to determine the levels of cyclohexenone derivatives (Schliemann et al., 2008a). For mycorradicin derivative quantification, 300 μL of the methanolic extracts was adjusted with potassium hydroxide to a final concentration of 0.5 M and processed as described (Fester et al., 2002a; Floss et al., 2008). Compounds were detected at 245 nm (cyclohexenone derivatives) or 377 nm (mycorradicin and its derivatives) and quantified by the external standards ABA and mycorradicin dimethyl ester.

The separation of C_{27} apocarotenoids in methanolic extracts was carried out in a similar manner on a 5-μm nucleosil C18 column (250 × 4 mm i.d.; Macherey-Nagel) using a solvent system consisting of solvent A (1.5% [v/v] aqueous H_3PO_4)/solvent B (acetonitrile) and a constant gradient from 0% B to 100% B (in A + B) within 60 min. Alkaline hydrolysis was done as described for mycorradicin, and reaction products were separated by applying a constant gradient from 0% to 100% B within 35 min followed by a 4-min hold and a rapid switch to 0% B within 1 min. For semipreparative HPLC, 1.5% aqueous H_3PO_4 was replaced by 2% formic acid and by a gradient raising solvent B from 0% to 100% within 35 min.

The high-resolution ESI mass spectra (ESI-FTICR-MS) of fractions Apo1 and Apo2 isolated after alkaline hydrolysis were obtained from a Bruker Apex III Fourier transform ion cyclotron resonance mass spectrometer (Bruker Daltonics) equipped with an Infinity cell, a 7.0-tesla superconducting magnet (Bruker), a radiofrequency-only hexapole ion guide, and an Apollo electrospray ion source (Agilent; off axis spray). Nitrogen was used as a drying gas at 150°C. The sample solutions were introduced continuously via a syringe pump with a flow rate of 120 μL h^{-1}. The *m/z* value obtained for Apo2 was 733.37944 $[M + H]^+$, calculated for $C_{39}H_{57}O_{13}^+$ 733.37937.

The positive ion ESI mass spectra of Apo2 were obtained from a Finnigan MAT TSQ Quantum Ultra AM system equipped with a hot ESI source (electrospray voltage, 3.0 kV; sheath gas, nitrogen; vaporizer temperature, 50°C; capillary temperature, 250°C). The MS system was coupled with a Surveyor Plus Micro-HPLC (Thermo Electron) equipped with a Ultrasep ES RP18E column (5 μm, 1 × 100 mm; SepServ). For HPLC, a gradient system was used starting from solvent C (90% water/10% acetonitrile, each of them containing 0.2% acetic acid) to solvent D (5% water/95% acetonitrile) within 15 min followed by a hold at 5% water/95% acetonitrile for a further 15 min with a flow rate of 50 μL min^{-1}. The CID mass spectra of Apo2 $[M + H]^+$ ions at *m/z* 733 (retention time, 19.7 min) were recorded during the HPLC run with collision energies of 15 and 25 eV, respectively (collision gas, argon; collision pressure, 1.5 mTorr).

For Apo2: 15-eV ESI-CID mass spectrum [*m/z*, relative intensity (%)]: 733 $[M + H]^+$ (10), 715 (8), 571 ($[M + H - C_6H_{10}O_5$ (hexose moiety)$]^+$ (22), 553 (8), 409 ($[M + H - 2 \times C_6H_{10}O_5]^+$ (75), 391 $[M + H - 2 \times C_6H_{10}O_5 - H_2O]^+$ (100), 373 (8).

For Apo2: 25-eV ESI-CID mass spectrum [*m/z*, relative intensity (%)]: 733 $[M + H]^+$ (7), 409 ($[M + H - 2 \times 162$ (hexose moiety)$]^+$ (43), 391$[M + H - 2 \times 162\text{-}H_2O]^+$ (29), 291 (17), 269 (100), 210 (47), 209 (29), 201 (61), 187 (41), 185 (35), 145 (12).

Root Staining Procedures and Microscopic Evaluation of Fungal Structures

Root fractions from a defined part of the root systems (center) were stained by 5% ink (Sheaffer skrip jet black; Sheaffer Manufacturing) in 2% acetic acid (Vierheilig et al., 1998). Root colonization, fungal structures, and arbuscule abundance were assessed using a stereomicroscope. The results were evaluated using the software Mycocalc according to Trouvelot et al. (1986). For experiment I, additional root aliquots were stained with 0.01% acid-fuchsin in lactoglycerol (lactic acid:glycerol:water, 1:1:1 [v/v/v]). Further details of subsequent visualization and classification of fungal arbuscules by confocal scanning microscopy (LSM 510 Meta; Zeiss) using the 543-nm laser line for excitation have been described elsewhere (Floss et al., 2008).

Real-Time RT-PCR

Total RNA was prepared using the Qiagen RNeasy Plant Mini Kit followed by DNase digestion (RNase-free DNase Set; Qiagen). RNA (1 μg) was reverse transcribed into cDNA with M-MLV Reverse Transcriptase RNase H Minus, Point Mutant (Promega) using oligo(dT) 19 primers. Real-time RT-PCR assays were performed using a SYBR Green-based kit according to the manufacturer's protocol (Applied Biosystems). Five nanograms of reverse-transcribed cDNA and 100 nM primers were used and assayed in a Mx 3005P QPCR system (Stratagene) using conditions and primer sets recently described (Floss et al., 2008). Briefly, the primer information for the four most important genes is given here: MtCCD1-qPCR-fw, 5′-TTCGGTGTTCTACCCCGCTAT-3′; MtCCD1-qPCR-re, 5′-AGGCGGCATGTGATCAAAC-3′; MtDXS2-1-qPCR-fw, 5′-CACCTTGGATACATAAATCATTAAGTC-3′; MtDXS2-1-qPCR-re, 5′-CGAATCTCTTCTCTCAACCAAGA-3′; MtEF-qPCR-fw, 5′-AGAAGGAAGCTGCTGAGATGAAC-3′; MtEF-qPCR-re, 5′-TGACTGTGCAGTAGTACTTGGTG-3′; MtPT4-qPCR-fw, 5′-ACAAATTTGATAGGATTCTTTTGCACGT-3′; MtPT4-qPCR-re, 5′-TCACATCTTCTCAGTTCTTGAGTC-3′.

The relative transcription ($E^{\Delta Ct}$) was calculated by subtracting the Ct values of the target gene from the arithmetic mean cycle threshold (Ct) value of the normalizing translation elongation factor of *M. truncatula* (MtEF) obtained

from three technical replicates. The efficiency of each PCR was determined by import of the fluorescence data into the LinReg PCR software (Ramakers et al., 2003).

Statistical Analysis

Data were evaluated for normal distribution and, if positive, a one-way test was performed, which at homogeneity of variance corresponds to ANOVA. If data did not comply with a normal distribution, the Kruskal-Wallis test was applied. The graphs show mean and SD values of individual transgenic root systems transformed by EV or the RNAi constructs of single composite plants.

Sequence data from this article can be found in the GenBank/EMBL data libraries under accession number FM204879 (MtCCD1).

Supplemental Data

The following materials are available in the online version of this article.

Supplemental Figure S1. Alignment of amino acid sequences from 14 plant CCD1 proteins, including MtCCD1.

ACKNOWLEDGMENTS

We thank M.J. Harrison (Boyce Thompson Institute) for providing the *M. truncatula* cDNA library; R. Geurts (Wageningen University) for providing pRedRoot and pRNAi; C. Rameau (INRA) for providing pea *rms5* mutant seeds, and H. Bothe (Cologne University) for providing the mycorradicin dimethyl ester standard. The skillful technical assistance of K. Manke and C. Kuhnt (Leibniz-Institut für Pflanzenbiochemie) is gratefully acknowledged.

Received June 20, 2008; accepted September 8, 2008; published September 12, 2008.

LITERATURE CITED

Akiyama K (2007) Chemical identification and functional analysis of apocarotenoids involved in the development of arbuscular mycorrhizal symbiosis. Biosci Biotechnol Biochem **71:** 1405–1414

Akiyama K, Matsuzaki KI, Hayashi H (2005) Plant sesquiterpenes induce hyphal branching in arbuscular mycorrhizal fungi. Nature **435:** 824–827

Alder A, Holdermann I, Beyer P, Al-Babili S (2008) Carotenoid oxygenases involved in plant branching catalyze a highly specific, conserved apocarotenoid cleavage reaction. Biochem J (in press)

Alexander T, Meier R, Toth R, Weber HC (1988) Dynamics of arbuscule development and degeneration in mycorrhizas of *Triticum aestivum* L. and *Avena sativa* L. with reference to *Zea mays* L. New Phytol **110:** 363–370

Auldridge ME, Block A, Vogel JT, Dabney-Smith C, Mila I, Bouzayen M, Magallanes-Lundback M, DellaPenna D, McCarty DR, Klee HJ (2006a) Characterization of three members of the Arabidopsis carotenoid cleavage dioxygenase family demonstrates the divergent roles of this multifunctional enzyme family. Plant J **45:** 982–993

Auldridge ME, McCarty DR, Klee HJ (2006b) Plant carotenoid cleavage oxygenases and their apocarotenoid products. Curr Opin Plant Biol **9:** 315–321

Booker J, Auldridge M, Wills S, McCarty D, Klee H, Leyser O (2004) MAX3/CCD7 is a carotenoid cleavage dioxygenase required for the synthesis of a novel plant signaling molecule. Curr Biol **14:** 1232–1238

Booker J, Sieberer T, Wright W, Williamson L, Willett B, Stirnberg P, Turnbull C, Srinivasan M, Goddarad P, Leyser O (2005) MAX1 encodes a cytochrome P450 family member that acts downstream of MAX3/4 to produce a carotenoid-derived branch-inhibiting hormone. Dev Cell **8:** 443–449

Bouvier F, Isner JC, Dogbo O, Camara B (2005) Oxidative tailoring of carotenoids: a prospect towards novel functions in plants. Trends Plant Sci **10:** 187–194

Bouvier F, Suire C, Mutterer J, Camara B (2003) Oxidative remodeling of chromoplast carotenoids: identification of the carotenoid dioxygenase CsCCD and CsZCD genes involved in *Crocus* secondary metabolite biogenesis. Plant Cell **15:** 47–62

Cooper CM, Davies NW, Menary RC (2003) C-27 apocarotenoids in the flowers of *Boronia megastigma* (Nees). J Agric Food Chem **51:** 2384–2389

Cunningham FX Jr, Gantt E (2001) One ring or two? Determination of ring number in carotenoids by lycopene ε-cyclases. Proc Natl Acad Sci USA **98:** 2905–2910

Cunningham FX Jr, Pogson B, Sun Z, McDonald KA, DellaPenna D, Gantt E (1996) Functional analysis of the β- and ε-lycopene cyclase enzymes of *Arabidopsis* reveals a mechanism for control of cyclic carotenoid formation. Plant Cell **8:** 1613–1626

Eugster CH, Märki-Fischer E (1991) The chemistry of rose pigments. Angew Chem Int Ed Engl **30:** 654–672

Fester T, Hause B, Schmidt D, Halfmann K, Schmidt J, Wray V, Hause G, Strack D (2002a) Occurrence and localization of apocarotenoids in arbuscular mycorrhizal plant roots. Plant Cell Physiol **43:** 256–265

Fester T, Schmidt D, Lohse S, Walter MH, Giuliano G, Bramley PM, Fraser PD, Hause B, Strack D (2002b) Stimulation of carotenoid metabolism in arbuscular mycorrhizal roots. Planta **216:** 148–154

Fester T, Wray V, Nimtz M, Strack D (2005) Is stimulation of carotenoid biosynthesis in arbuscular mycorrhizal roots a general phenomenon? Phytochemistry **66:** 1781–1786

Floss DS, Hause B, Lange PR, Küster H, Strack D, Walter MH (2008) Knock-down of the MEP pathway isogene *1-deoxy-D-xylulose 5-phosphate synthase 2* inhibits formation of arbuscular mycorrhiza-induced apocarotenoids and abolishes normal expression of mycorrhiza-specific plant marker genes. Plant J **56:** 86–100

Frenzel A, Manthey K, Perlick AM, Meyer F, Pühler A, Küster H, Krajinski F (2005) Combined transcriptome profiling reveals a novel family of arbuscular mycorrhizal-specific *Medicago truncatula* lectin genes. Mol Plant Microbe Interact **18:** 771–782

Giuliano G, Al-Babili S, von Lintig J (2003) Carotenoid oxygenases: cleave it or leave it. Trends Plant Sci **8:** 145–149

Gomez-Roldan V, Fermas S, Brewer PB, Puech-Pagès V, Dun EA, Pillot JP, Letisse F, Matusova R, Danoun S, Portais JC, et al (2008) Strigolactone inhibition of shoot branching. Nature **455:** 189–194

Hans J, Hause B, Fester T, Strack D, Walter MH (2004) Cloning, characterization and immunolocalization of a mycorrhiza-inducible 1-deoxy-D-xylulose 5-phosphate isomerase in arbuscule-containing cells of maize. Plant Physiol **134:** 614–624

Harrison MJ, Dewbre GR, Liu J (2002) A phosphate transporter from *Medicago truncatula* involved in the acquisition of phosphate released by arbuscular mycorrhizal fungi. Plant Cell **14:** 2413–2429

Hirschberg J (2001) Carotenoid biosynthesis in flowering plants. Curr Opin Plant Biol **4:** 210–218

Hohnjec N, Vieweg MF, Pühler A, Becker A, Küster H (2005) Overlaps in the transcriptional profiles of *Medicago truncatula* roots inoculated with two different *Glomus* fungi provide insights into the genetic program activated during arbuscular mycorrhiza. Plant Physiol **137:** 1283–1301

Huhman DV, Berhow MA, Sumner LW (2005) Quantification of saponins in aerial and subterranean tissues of *Medicago truncatula*. J Agric Food Chem **53:** 1914–1920

Huhman DV, Sumner LW (2002) Metabolic profiling of saponins in *Medicago sativa* and *Medicago truncatula* using HPLC coupled to an electrospray ion-trap mass spectrometer. Phytochemistry **59:** 347–360

Ibdah M, Azulay Y, Portnoy V, Wasserman B, Bar E, Meir A, Burger Y, Hirschberg J, Schaffer AA, Katzir N, et al (2006) Functional characterization of CmCCD1, a carotenoid cleavage dioxygenase from melon. Phytochemistry **67:** 1579–1589

Javot H, Penmetsa RV, Terzaghi N, Cook DR, Harrison MJ (2007) A *Medicago truncatula* phosphate transporter indispensable for the arbuscular mycorhizal symbiosis. Proc Natl Acad Sci USA **104:** 1720–1725

Johnson X, Brcich T, Dun EA, Goussot M, Haurogné K, Beveridge CA, Rameau C (2006) Branching genes are conserved across species: genes controlling a novel signal in pea are coregulated by other long-distance signals. Plant Physiol **142:** 1014–1026

Kato M, Matsumoto H, Ikoma Y, Okuda H, Yano M (2006) The role of carotenoid cleavage dioxygenases in the regulation of carotenoid profiles during maturation of citrus fruit. J Exp Bot **57:** 2153–2164

Klingner A, Bothe H, Wray V, Marner FJ (1995) Identification of a yellow pigment formed in maize roots upon mycorrhizal colonization. Phytochemistry **38:** 53–55

Kloer DP, Schulz GE (2006) Structural and biological aspects of carotenoid cleavage. Cell Mol Life Sci **63:** 2291–2303

Kuhn R, Brockmann H (1935) Über den stufenweisen Abbau und die Konstituion des β-Carotins. Liebigs Ann Chem **516:** 95–143

Lewinsohn E, Sitrit Y, Bar E, Azulay Y, Ibdah M, Meir A, Yosef E, Zamir D, Tadmor Y (2005) Not just colors: carotenoid degradation as a link between pigmentation and aroma in tomato and watermelon fruit. Trends Food Sci Technol **16:** 407–415

Limpens E, Ramos J, Franken C, Raz V, Compaan B, Fransen H, Bisseling T, Geurts R (2004) RNA interference in *Agrobacterium rhizogenes*-transformed roots of *Arabidopsis* and *Medicago truncatula*. J Exp Bot **55:** 983–992

Lohse S, Schliemann W, Ammer C, Kopka J, Strack D, Fester T (2005) Organization and metabolism of plastids and mitochondria in arbuscular mycorrhizal roots of M*edicago truncatula*. Plant Physiol **139:** 329–340

Maier W, Peipp H, Schmidt J, Wray V, Strack D (1995) Levels of a terpenoid glycoside (blumenin) and cell wall-bound phenolics in some cereal mycorrhizas. Plant Physiol **109:** 465–470

Marasco EK, Vay K, Schmidt-Dannert, C (2006) Identification of carotenoid cleavage dioxygenases from Nostoc sp. PCC7120 with different cleavage activities. J Biol Chem **281:** 31583–31593

Mathieu S, Terrier N, Procureur J, Bigey F, Günata Z (2005) A carotenoid cleavage dioxygenase from *Vitis vinifera* L.: functional characterization and expression during grape berry development in relation to C_{13}-norisoprenoid accumulation. J Exp Bot **56:** 2721–2731

Matusova R, Rani K, Verstappen FWA, Franssen MCR, Beale MH, Bouwmeester H (2005) The strigolactone germination stimulants of the plant parasitic *Striga* and *Orobanche* spp. are derived from the carotenoid pathway. Plant Physiol **139:** 920–934

Mouchel CF, Leyser O (2007) Novel phytohormones involved in long-range signaling. Curr Opin Plant Biol **10:** 473–476

Nambara E, Marion-Poll A (2005) Abscisic acid biosynthesis and catabolism. Annu Rev Plant Biol **56:** 165–185

Ohmiya A, Kishimoto S, Aida R, Yoshioka S, Sumimoto K (2006) Carotenoid cleavage dioxygenase (CmCCD4a) contributes to white color formation in chrysanthemum petals. Plant Physiol **142:** 1193–1201

Ramakers C, Ruijter JM, Lekanne Deprez RH, Moormann FM (2003) Assumption-free analysis of quantitative real-time polymerase chain reaction (PCR) data. Neurosci Lett **339:** 62–66

Rodríguez-Concepción M, Boronat A (2002) Elucidation of the methylerythritol phosphate pathway for isoprenoid biosynthesis in bacteria and plastids: a metabolic milestone achieved through genomics. Plant Physiol **130:** 1079–1089

Rubio A, Rambla JL, Santaella M, Gómez MD, Orzaez D, Granell A, Gómez-Gómez L (2008) Cytosolic and plastoglobule targeted carotenoid dioxygenases from *Crocus sativus* are both involved in β-ionone-release. J Biol Chem **283:** 24816–24825

Scherzinger D, Al-Babili S (2008) In vitro characterization of a carotenoid cleavage dioxygenase from *Nostoc* sp. PCC 7120 reveals a novel cleavage pattern, cytosolic localization and induction by high light. Mol Microbiol **69:** 231–244

Schliemann W, Ammer C, Strack D (2008a) Metabolite profiling of mycorrhizal roots of *Medicago truncatula*. Phytochemistry **69:** 112–146

Schliemann W, Kolbe B, Schmidt J, Nimtz M, Wray V (2008b) Accumulation of apocarotenoids in mycorrhizal roots of leek (*Allium porrum*). Phytochemistry **69:** 1680–1688

Schmidt H, Kurtzer R, Eisenreich W, Schwab W (2006) The carotenase AtCCD1 from *Arabidopsis thaliana* is a dioxygenase. J Biol Chem **281:** 9845–9851

Schwartz SH, Qin X, Loewen MC (2004) The biochemical characterization of two carotenoid cleavage enzymes from Arabidopsis indicates that a carotenoid-derived compound inhibits lateral branching. J Biol Chem **279:** 46940–46945

Schwartz SH, Qin X, Zeevaart JA (2001) Characterization of a novel carotenoid cleavage dioxygenase from plants. J Biol Chem **276:** 25208–25211

Schwartz SH, Tan BC, Gage DA, Zeevaart JA, McCarty DR (1997) Specific oxidative cleavage of carotenoids by VP14 of maize. Science **276:** 1872–1874

Simkin AJ, Schwartz SH, Auldridge M, Taylor MG, Klee HJ (2004a) The tomato carotenoid cleavage dioxygenase 1 genes contribute to the formation of the flavor volatiles β-ionone, pseudoionone, and geranylacetone. Plant J **40:** 882–892

Simkin AJ, Underwood BA, Auldridge M, Loucas HM, Shibuya K, Schmelz E, Clark DG, Klee HJ (2004b) Circadian regulation of the PhCCD1 carotenoid cleavage dioxygenase controls emission of β-ionone, a fragrance volatile of petunia flowers. Plant Physiol **136:** 3504–3514

Snowden KC, Simkin AJ, Janssen BJ, Templeton KR, Loucas HM, Simons JL, Karunairetnam S, Gleave AP, Clark DG, Klee HJ (2005) The decreased apical dominance1 *Petunia hydrida* CAROTENOID CLEAVAGE DIOXYGENASE8 gene affects branch production and plays a role in leaf senescence, root growth, and flower development. Plant Cell **17:** 746–759

Strack D, Fester T (2006) Isoprenoid metabolism and plastid reorganization in arbuscular mycorrhizal roots. New Phytol **172:** 22–34

Sun Z, Gantt E, Cunningham FX Jr (1996) Cloning and functional analysis of the β-carotene hydroxylase of *Arabidopsis thaliana*. J Biol Chem **271:** 24349–24352

Sun Z, Hans J, Walter MH, Matusova R, Beekwilder J, Verstappen FWA, Ming Z, van Echtelt E, Strack D, Bisseling T, et al (2008) Cloning and characterisation of a maize carotenoid cleavage dioxygenase (*ZmCCD1*) and its involvement in the biosynthesis of apocarotenoids with various roles in mutualistic and parasitic interactions. Planta **228:** 789–801

Tan BC, Joseph LM, Deng WT, Liu L, Li QB, Cline K, McCarty DR (2003) Molecular characterization of the Arabidopsis 9-*cis* epoxycarotenoid dioxygenase gene family. Plant J **35:** 44–56

Trouvelot A, Kough JL, Gianinazzi-Pearson V (1986) Mesure du taux de mycorhization VA d'un système radiculaire: recherche des méthodes d'estimation ayant une signification fonctionnelle. *In* V Gianinazzi-Pearson, S Gianinazzi, eds, The Mycorrhizae: Physiology and Genetics. INRA Presse, Paris, pp 217–221

Umehara M, Hanada A, Yoshida S, Akiyama K, Arite T, Takeda-Kamiya N, Magome H, Kamiya Y, Shirasu K, Yoneyama K, et al (2008) Inhibition of shoot branching by new terpenoid plant hormones. Nature **455:** 195–200

Vierheilig H, Coughlan AP, Wyss U, Piché Y (1998) Ink and vinegar, a simple staining technique for arbuscular-mycorrhizal fungi. Appl Environ Microbiol **64:** 5004–5007

Vogel JT, Tan BC, McCarty DR, Klee HJ (2008) The carotenoid cleavage dioxygenase 1 enzyme has broad substrate specificity, cleaving multiple carotenoids at two different bond positions. J Biol Chem **283:** 11364–11373

Walter MH, Fester T, Strack D (2000) Arbuscular mycorrhizal fungi induce the non-mevalonate methylerythritol phosphate pathway of isoprenoid biosynthesis correlated with the accumulation of the 'yellow pigment' and other apocarotenoids. Plant J **21:** 571–578

Walter MH, Floss DS, Hans J, Fester T, Strack D (2007) Apocarotenoid biosynthesis in arbuscular mycorrhizal roots: contributions from methylerythritol phosphate pathway isogenes and tools for its manipulation. Phytochemistry **68:** 130–138

Walter MH, Hans J, Strack D (2002) Two distantly related genes encoding 1-deoxy-D-xylulose 5-phosphate synthases: differential regulation in shoots and apocarotenoid-accumulating mycorrhizal roots. Plant J **31:** 243–254

Yokoyama H, White MJ (1966) Citrus carotenoids. VI. Carotenoid pigments in the flavedo of Sinton citrangequat. Phytochemistry **5:** 1159–1173

Ytterberg AJ, Peltier JP, van Wijk K (2006) Protein profiling of plastoglobules in chloroplasts and chromoplasts: a surprising site for differential accumulation of metabolic enzymes. Plant Physiol **140:** 984–997

Zou J, Zhang S, Zhang W, Li G, Chen Z, Zhai W, Zhao X, Pan X, Xie Q, Zhu L (2006) The rice HIGH-TILLERING DWARF1 encoding an ortholog of the *Arabidopsis* MAX3 is required for negative regulation of the outgrowth of axillary buds. Plant J **48:** 687–696